machines

MDPI

Article

A Study on the Design of a Variable Power Electromagnetic Brake for Industrial Applications

Ye-Ji Park [1], Jae-Kwang Lee [2], Ki-Doek Lee [2] and Dong-Hoon Jung [3,*]

[1] ECL-TECH Corp., Engineering Center 606, 222 Wangsimni-ro, Seongdoong-gu, Seoul 04763, Republic of Korea; yejip94@gmail.com
[2] Intelligent Mechatronics Research Center, Korea Electronics Technology Institute, Bucheon 14502, Republic of Korea; leejk@keti.re.kr (J.-K.L.); kdlee@keti.re.kr (K.-D.L.)
[3] Department of Electrical Engineering, Andong National University, Andong 36729, Republic of Korea
* Correspondence: dhjung@anu.ac.kr

Abstract: This paper discusses a permanent-magnet electromagnetic brake for the semiconductor process of hollow integrated modules. This permanent-magnet electromagnetic brake is characterized by permanent magnets arranged at the bottom of the stator and coils positioned in the middle portion of the stator. The attractive force is generated by the magnetic energy from the permanent magnet, and to counteract the holding force, a current must be applied to the coils. In the case of a permanent-magnet electromagnetic brake, the maximum holding force that can be generated is fixed by the permanent magnet inserted at the bottom, and even if the load conditions vary, the holding force cannot be altered. This study investigated a method to secure an additional holding force by inducing iron losses at the moment when the holding force is required through improvements in the structure of both the stator and rotor of a permanent-magnet electromagnetic brake. To validate the feasibility of this study, prototypes of permanent-magnet brakes were fabricated, and dynamometer tests were conducted.

Keywords: electromagnetic brake; permanent magnet; holding force; attractive force; slit alignment

check for updates

Academic Editor: Ahmed Abu-Siada

Received: 8 January 2025
Revised: 19 February 2025
Accepted: 19 February 2025
Published: 24 February 2025

Citation: Park, Y.-J.; Lee, J.-K.; Lee, K.-D.; Jung, D.-H. A Study on the Design of a Variable Power Electromagnetic Brake for Industrial Applications. *Machines* **2025**, *13*, 181. https://doi.org/10.3390/machines13030181

Copyright: © 2025 by the authors. Licensee MDPI, Basel, Switzerland. This article is an open access article distributed under the terms and conditions of the Creative Commons Attribution (CC BY) license (https://creativecommons.org/licenses/by/4.0/).

1. Introduction

Electromagnetic brakes are widely utilized in various industrial sectors, including military applications, robotics, healthcare, cranes, and forklifts, because they can effectively meet the demands of industrial operations [1]. Existing electromagnetic brakes can be classified into electromagnetic and permanent-magnet types. In the electromagnetic-type, coils are inserted into the stator core, and when a holding force is required, a current is applied. When the current flows, a magnetic flux is generated in the stator, inducing eddy currents in the rotor, and thus accumulating magnetic energy in the air gap. This generates an attractive force that is converted into a holding force between the stator and rotor [2–4].

In the permanent-magnet electromagnetic brake discussed in this paper, permanent magnets are arranged at the bottom of the stator, with coils positioned in the middle part of the stator [5–8]. Continuous research has been conducted on designs leveraging the magnetization direction of the permanent magnets and enhancing the braking force [9–11]. An attractive force is generated by the magnetic energy from the permanent magnet, and to counteract the holding force, a current must be applied to the coils. Depending on the operating environment and load, the efficiency of the permanent-magnet electromagnetic

brake system may be higher than that of electromagnetic brakes [12]. However, in conventional permanent-magnet electromagnetic brakes, the maximum holding force that can be generated is determined by the permanent magnet inserted at the bottom, and even if the load conditions vary, the holding force cannot be altered. This results in unnecessary energy consumption under light loads [13].

Various studies have been conducted to enhance the performance of electromagnetic braking systems. These include developing analytical models and designing electromagnetic brakes through 3D modeling [14], considering the key design parameters of the coil inside the brake [15] and incorporating physical control mechanisms to achieve precise braking performance [16]. However, research on hybrid electromagnetic brakes that integrate electromagnets and permanent magnets is extremely limited. Therefore, this study proposes an electromagnetic brake that combines electromagnets and permanent magnets, which improves the system performance by enabling an adjustable holding force and inducing iron losses.

This paper provides an overview of the principles and design methods of permanent-magnet electromagnetic brakes. In this work, the basic design process was simplified by geometrically defining the key design parameters for each part. Additionally, research was conducted on methods to obtain variable output and improve the efficiency of permanent-magnet electromagnetic brake systems. A method is proposed to secure an additional holding force by inducing iron losses at the moment when a holding force is required. This is achieved through improvements in the structure of both the stator and rotor that allow for variable power. Iron losses occur because of the changes in magnetic flux over time, and intentionally inducing iron losses by incorporating a slotted structure in the stator and rotor enhances the holding force. Furthermore, the system efficiency is improved by utilizing the magnetization and demagnetization phenomena based on the load conditions. By employing AlNiCo magnets with low coercivity, demagnetization of the permanent magnets can be induced, enabling their application in variable-speed brake systems. Heat loss is an inherent challenge when controlling braking force using permanent magnets, and extensive research efforts are continuously being made to address this problem effectively [17–19]. The slotted structure acts as an external air duct for cooling the coils, improving the cooling performance and, as mentioned earlier, enhancing the holding force through iron losses. Finally, to validate the feasibility of the methods proposed in this research, prototypes of permanent magnet brakes were manufactured and dynamometer tests were conducted. Figure 1 shows a manufacturing model of a brake and motor used in industrial equipment. The brake used in this study was located at the front of the motor.

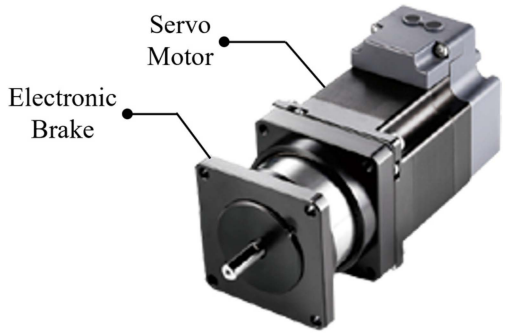


Figure 1. Configuration of electromagnetic brake-integrated industrial motor.

2. Permanent Magnet-Type Electromagnetic Brake Design Method

2.1. Brake Design and Operating Principle

The electromagnetic brake generates a braking force through the attractive force of the magnetic flux generated from the permanent magnet located in the stator, and is driven in such a way that the magnetic flux of the permanent magnet is offset by the application of current during operation. To calculate the required holding force for brake design, it is necessary to determine the required attractive force using the effective area and friction coefficient of the brake contact surface. Figure 2 illustrates the relationship between the holding and attractive forces. R_o and R_i are the outer and inner radii of the contact surface, respectively. The effective radius, R_{eff} is derived from the inner and outer radii. When the brake is activated, an attractive force is generated. This attractive force is multiplied by the friction coefficient of the brake pads to produce a frictional force. Consequently, the braking torque is determined by the product of the forces on both sides and the distance between the pads and center of rotation. Therefore, the braking torque can be expressed as shown in Equation (3). Equations (1)–(3) illustrate the process of deriving the braking torque T_b using the effective radius and coefficient of friction. μ_s is the coefficient of friction of the brake pad, and N is the attractive force required to generate the braking torque [20].

$$R_{eff} = \frac{R_o - R_i}{2} \, [m] \tag{1}$$

$$F = \mu_s N \, [N] \tag{2}$$

$$T_B = \mu_s N R_{eff} = \mu_s N \left(\frac{R_o - R_i}{2} \right) \, [Nm] \tag{3}$$

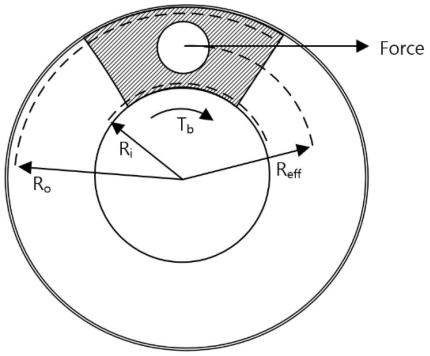


Figure 2. Relationship between holding force and attractive force.

2.2. Brake Design and Driving Principle

Figure 3 depicts the mechanical configuration of the permanent-magnet electromagnetic brake. In Figure 3, A is the brake pad, B is the coil, and C is the permanent magnet. It contains a rotor and stator, and the permanent magnet located at the bottom of the stator accumulates magnetic energy in the air gap, generating an attractive force. This attractive force is then converted into the holding force of the brake. When driving is required, the system is driven by applying a current to the coil located in the middle of the stator to counteract the magnetic flux generated by the permanent magnet.

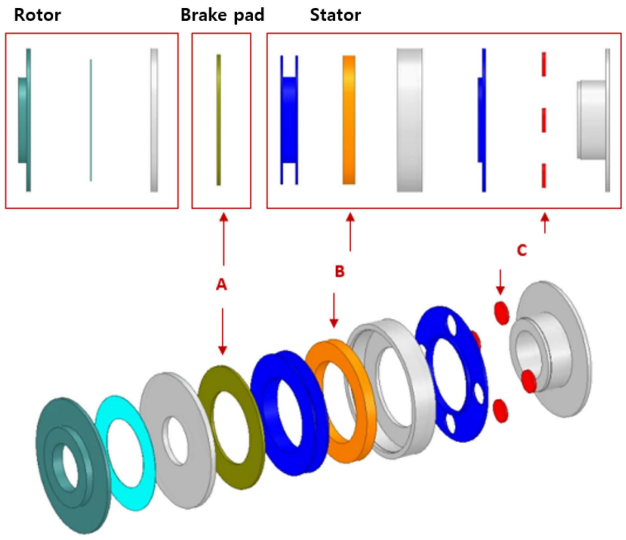


Figure 3. Hybrid-type electromagnetic brake configuration.

Figure 4 shows a schematic of the operating principle of the brake. In the figure, Figure 4a represents the case in which the holding force is generated by the magnetomotive force produced in the permanent magnet, and Figure 4b illustrates the concept of a state in which the current is applied to the coil to counteract the magnetomotive force of the permanent magnet. A permanent magnet is embedded at the bottom of the stator, and the magnetic flux generated by the permanent magnet forms a closed loop with the rotor passing through the stator core. This interaction generates an attractive force, which in turn produces a braking force. Conversely, to counteract the braking force during the operation, a current is applied to the winding located in the middle section of the stator. This current neutralizes the magnetic flux generated by the permanent magnet, thereby canceling the attractive force.

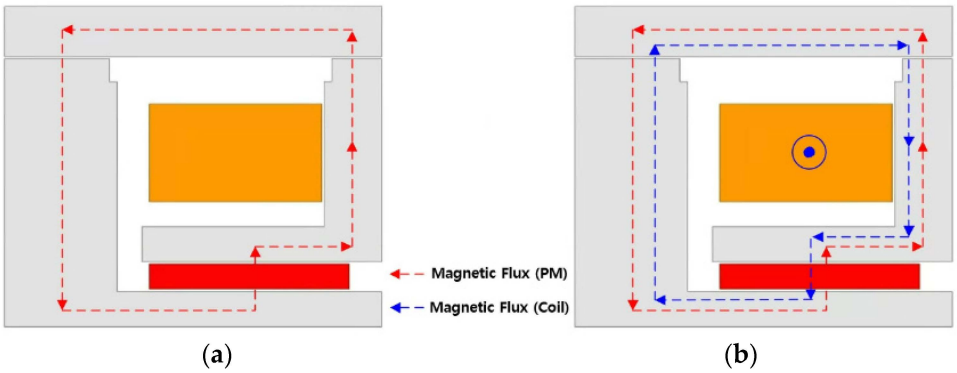


Figure 4. Permanent magnet-type electromagnetic brake-operating principle concept diagram (**a**) Magnetic flux by permanent magnet (**b**) Magnetic flux by permanent magnets and coils.

Figure 5 shows the results of simulating the phenomenon using 3D finite element analysis (FEA). In (a), the magnetic flux is distributed in both the stator and rotor, whereas (b) depicts the magnetic flux being neutralized by the current flowing through the coil. As shown in (b), the attractive force can be counteracted using the magnetic flux induced by the current.

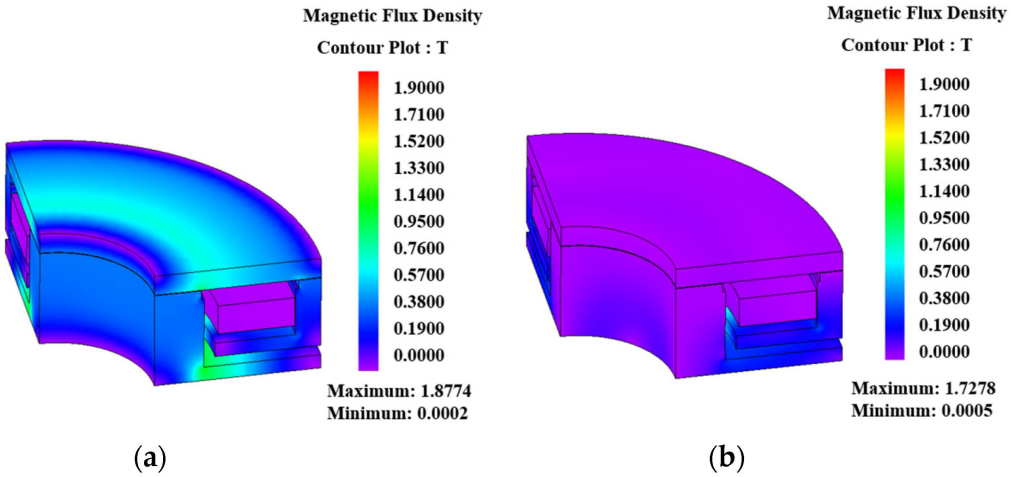


Figure 5. Three-dimensional electromagnetic field analysis using 3D FEA (**a**) no current field (**b**) current field.

Table 1 lists the specifications of the brake. The holding force that must be generated by the brake is 0.4 [Nm] considering the specified inner and outer diameter limits. A material with a friction coefficient of 0.4 is used for the brake pads located between the stator and rotor. Carbon steel, copper, and rare-earth permanent magnets were used.

Table 1. Specifications for design.

Contents	Value	Unit
Dia. Outer	60	mm
Dia. Inner	30	mm
Friction Factor	0.4	-
Brake Torque	0.4	Nm
Attractive Force	67	N

By utilizing the information provided in Table 1 and Equation (3), the attractive force required to be generated by the brake can be derived.

2.3. Hybrid-Type Electromagnetic Brake Design Algorithm

In this section, a design algorithm for a permanent-magnet electromagnetic brake is proposed. Figure 6 shows a schematic of the brake design algorithm.

As a first step, the design characteristics of the device, friction coefficients, and attractive force necessary to generate the target holding force were derived using the previously described equations. Next, for application to a wafer transfer robot, the current density considering the input voltage and cooling characteristics, as well as the current limit considering the controller specifications, were calculated. Using 3D FEA, the number of magnets located at the bottom of the stator capable of generating the target attractive force was determined. In the next phase of the coil design, the number of turns and the input current required to neutralize the magnetic flux generated by the permanent magnet were calculated. During this process, the design considered the input voltage, current saturation limits, and ratio of current to weight. The coil design was completed when the attractive force generated by the input current became smaller than the force created by the weight of the rotor. Finally, after confirming issues such as current and voltage limits and magnetic saturation, the design of the permanent-magnet-type electromagnetic brake was finalized.

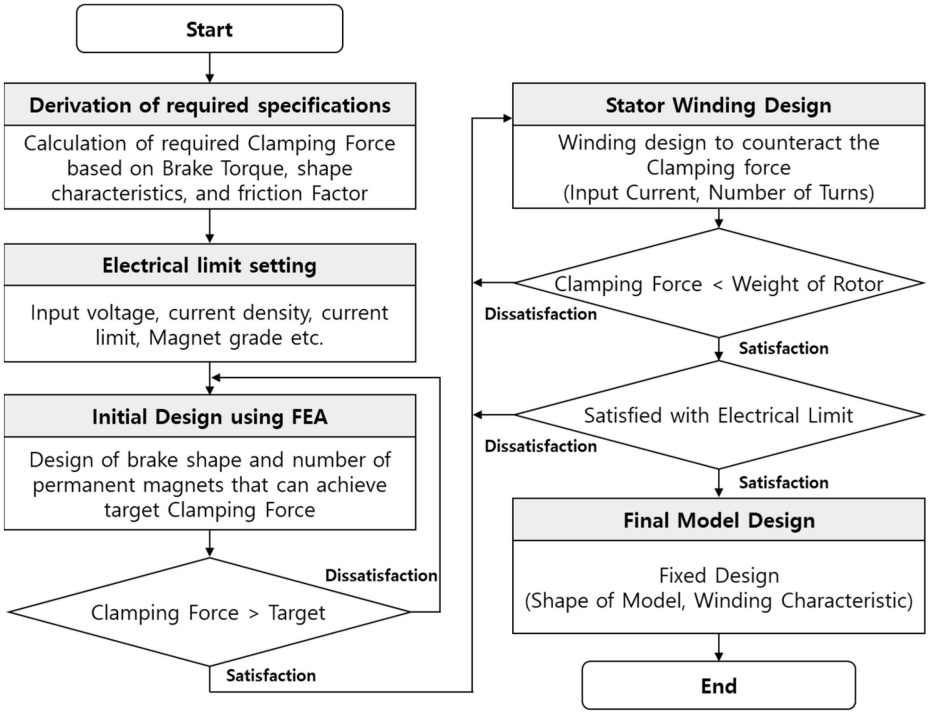


Figure 6. Hybrid-type electromagnetic brake design process.

Figure 7 illustrates the key design parameters of the electronic brake analyzed in this study. The design focuses on the thicknesses of the inner and outer yokes, thickness of the permanent magnet, and coil area.

No.	Contents
1	Width of inner yoke
2	Width of outer yoke
3, 4	Thickness of under yoke
5	Thickness of Magnet
6	Thickness of Rotor yoke
7	Area of Coil

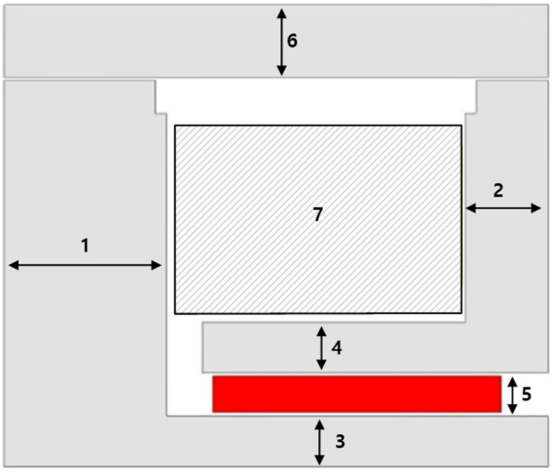


Figure 7. Main design variables for electromagnetic brakes.

3. Research on Improving the Characteristics of Permanent Magnet Electromagnetic Brakes

This section proposes a slit structure for the stator and rotor to improve the characteristics of permanent-magnet-type electromagnetic brakes. The slit structure exposed the coils to the outside, thereby enhancing the cooling performance. In addition, it induces iron loss between the stator and rotor, enabling the generation of additional braking torque.

3.1. Calculating Core Loss

The core loss occurring in the stator and rotor is generated by the temporal variation in the magnetic flux density and can be expressed by Equation (4), which represents the

characteristics of core loss by utilizing the temporal variation in the magnetic field and eddy current [21,22].

$$w_c = w_{ce} + w_{ch} = K_e f^2 B_{max} + K_h f B_{max}^2 \quad (4)$$

where w_{ce} and w_{ch} are the eddy current and hysteresis losses per weight, respectively; K_e and K_h are experimental constants obtained by the Epstein frame; f is the frequency of the alternating magnetic field; and B_{max} is the maximum flux density during the time interval.

However, when using a sinusoidal power input such as a motor, time harmonics occur. In addition, the direction of the magnetic field is not constant because of the rotating magnetic field. In this case, the core loss can be expressed using the Fourier transform of the magnetic flux density waveform at each point. The core loss at this time is expressed by Equation (5).

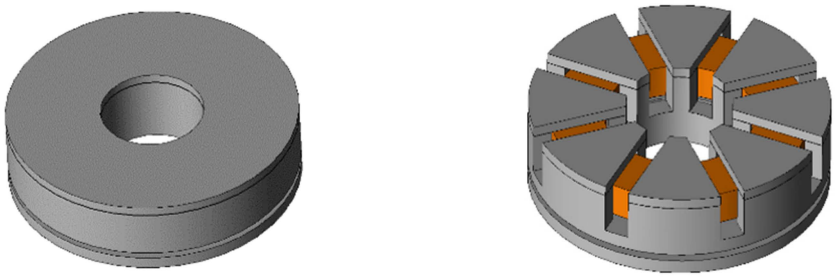
$$W_c = \int_{core} \sum_n K_e D(nf)^2 \cdot \left\{ B_{r,n}^2 + B_{\theta,n}^2 \right\} dv + \int_{core} \sum_n K_h D(nf) \cdot \left\{ B_{r,n}^2 + B_{\theta,n}^2 \right\} dv \quad (5)$$

where D is the density of the electrical steel plate, n is the time harmonic order, and $B_{r,n}$ and $B_{\theta,n}$ are the nth harmonics of the radial and peripheral components of the flux density.

The iron loss expressed in Equation (5) includes the sum of harmonic losses due to time harmonics. The magnetic fields caused by the eddy currents of the stator and rotor and the magnetic fields caused by the armature currents and magnets are ignored.

3.2. Improved Iron Loss Induction and Holding Force Through Slit Application

Figure 8 shows an example of a model with a slit applied to generate iron loss. Figure 8a shows a conventional electromagnetic brake, and Figure 8b depicts an electromagnetic brake with slits. When slits are applied to the rotor and stator, the inflow of external air is facilitated, improving the cooling performance, and the magnetic flux changes according to the movement of the rotor.

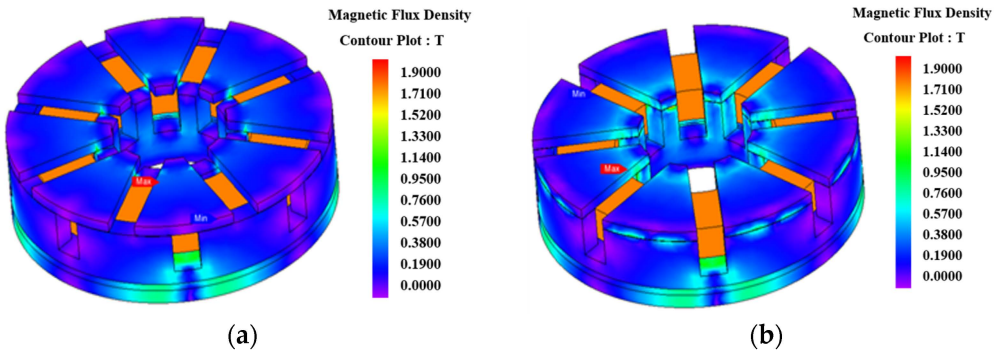


(**a**) (**b**)

Figure 8. Example of a model with slits applied (**a**) Structure without slots (**b**) Structure with slots.

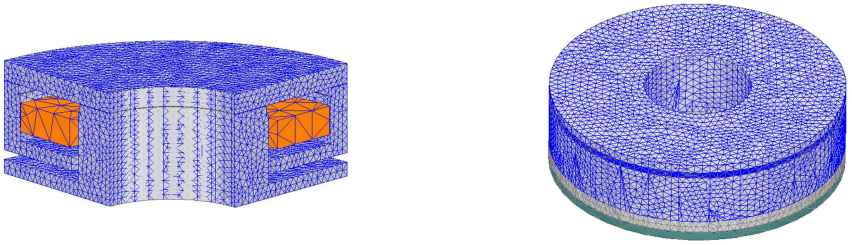
Figure 9 shows the change in the magnetic flux density when the stator and rotor slits are aligned or not. In Figure 9a, the slits of the stator and rotor are not aligned, the magnetic resistance generated by the slit between the stator and rotor magnetic paths is reduced, and the magnitude of the passing magnetic flux is reduced. In Figure 9b, the slits are aligned, the magnetic resistance between the stator and rotor paths is omitted, and the size of the passing magnetic flux is increased. This suggests that the iron loss may be generated by a change in the magnetic flux caused by rotation. The electromagnetic analysis software JMAG 22.2 and Maxwell 2023 R1 were utilized for this analysis. After analyzing the convergence of the results, more than 300,000 elements were used in the 3D electromagnetic FEA. The mesh of the analytical model is shown in Figure 10. Carbon steel, NdFeB, and Cu were used as the magnetic material, permanent magnet, and coil, respectively. For the convenience of analysis,

the boundary condition was divided into four parts, a Symmetry Boundary Condition was applied, and the external area was set to air.



(**a**) (**b**)

Figure 9. Magnetic flux density changes with and without slit alignment (**a**) Slits Are Misaligned (**b**) Slits Are Aligned.



(**a**) (**b**)

Figure 10. The mesh for the analysis model (**a**) Mesh of periodic model (**b**) Full model mesh.

3D FEA was used to check the braking torque according to the iron loss, and it was confirmed that a braking torque was generated, as shown in Figure 11. In this analysis, the pole pair was assumed to be two slits, and in the case of 720°, shown in Figure 11, it can be calculated as an angle that includes four slits. Because the slits are aligned at the initial position and the three slits rotate during the analysis cycle, excluding the slit at the initial position, it can be confirmed that three reverse torques occur.

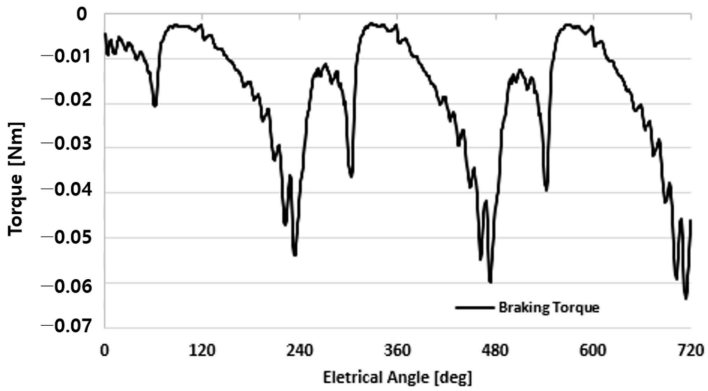


Figure 11. Analysis results of braking force through core loss induction.

3.3. Development of an Output Variable Electromagnetic Brake Using AlNiCo Magnets

AlNiCo permanent magnets can be employed to enhance the system efficiency by generating a variable braking force, as illustrated in Figure 12. Compared to NdFeB magnets, as shown in Figure 13, AlNiCo magnets have a lower coercivity and are thus easier to magnetize and demagnetize. This property enables the adjustment of the braking force in response to load variations.

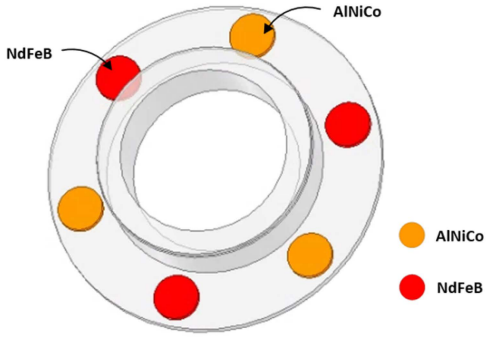


Figure 12. Examples of AlNiCo magnet applications.

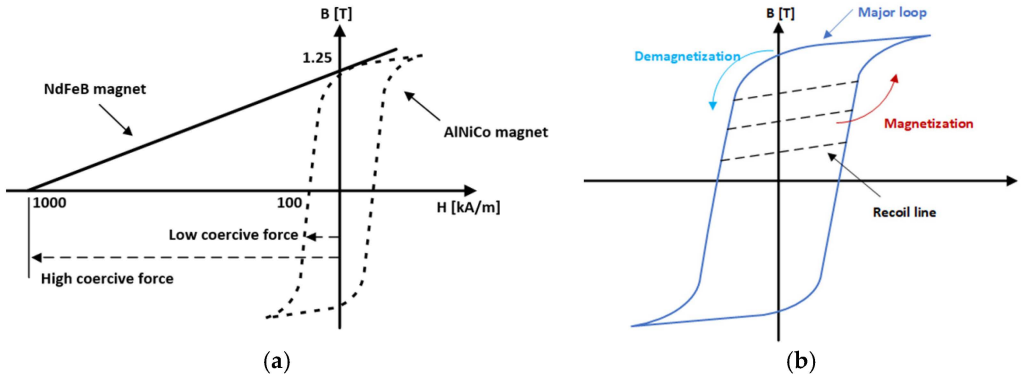


Figure 13. (**a**) AlNlico magnet and NdFeB characteristics; (**b**) AlNlico magnet magnetization and demagnetization.

When the required braking force decreases owing to changes in operating conditions, the braking force can be reduced by demagnetizing the AlNiCo magnets. This prevents the generation of excessive braking forces, thereby improving the durability of the brake pads. When offsetting the braking force is necessary, the magnetic flux of the permanent magnets can be neutralized by applying a current to the winding, as shown in Figure 14. In this figure, the x-axis represents the applied current, and the y-axis indicates the attractive force. By applying a current to the winding based on the load type, the magnetic flux of the permanent magnets can be completely canceled, thereby reducing the force to zero.

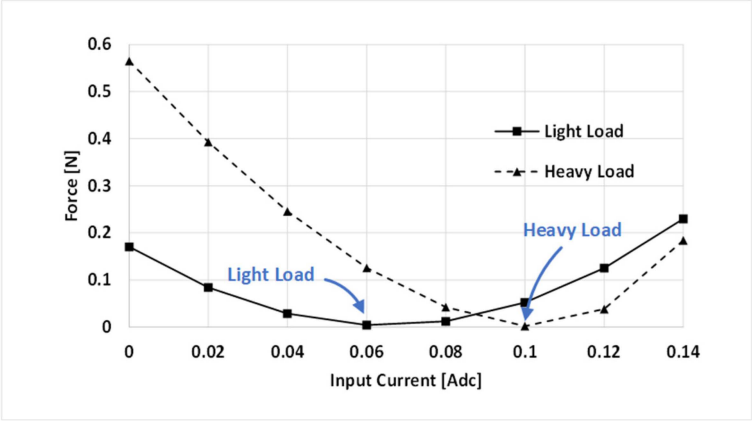


Figure 14. Current required to offset attractive force based on load conditions.

Furthermore, the attractive force can be varied by magnetizing or demagnetizing the permanent magnets, depending on the presence of heavy or light loads. Consequently,

the amount of current applied during rotor operation can also be adjusted. The system efficiency can be improved by varying the input current in accordance with the load conditions.

3.4. Verification Through Experimental Tests

Figure 15 shows the test environment of the manufactured electromagnetic brake. The test was conducted using an HBM.Co torque sensor, Siemens load motor, and Yaskawa power analyzer.

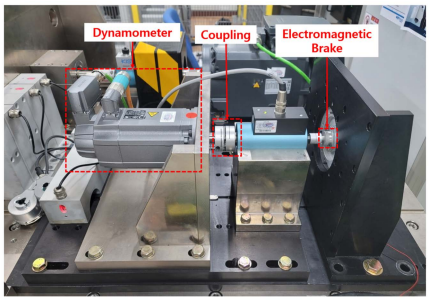


Figure 15. Electromagnetic brake examination environment.

4. Discussion

Conventional electronic brakes generate a holding force using permanent magnets. When the holding force needs to be reduced owing to changing operational conditions, a current must be applied to offset the magnetic flux generated by the permanent magnets. Consequently, even in cases where the holding force is reduced, an excessive amount of current is applied, leading to decreased system efficiency. The electronic brake proposed in this study can generate an appropriate holding force according to the operating conditions by demagnetizing the permanent magnets. As a result, significantly less current is required under light load conditions than under heavy load conditions, thereby improving the system efficiency.

A method is proposed that enhances the stator and rotor structures to control the variable output of a permanent-magnet-based electromagnetic brake. This method induces iron losses at critical moments when a holding force is required, thereby ensuring an additional holding force. A slit-structured design was derived, and its performance, including torque and output, was validated. Its efficiency was measured and verified using IEC 60034-2-1, an internationally recognized testing standard [23]. The proposed permanent-magnet-based electromagnetic brake design successfully achieved variable output control, satisfying the requirements for high-performance applications.

High driving efficiency and holding force of electronic brakes are critical performance requirements for joint robotic systems in high-precision robotics. A representative application is a semiconductor wafer transfer robot, which requires electronic brakes with such capabilities. The hybrid structure, which utilizes both electromagnets and permanent magnets, eliminates the need for an electric current to generate a holding force, as the permanent magnets provide a holding force based on the load conditions. Furthermore, a substantial holding force can be achieved by integrating high-performance permanent magnets. Additionally, incorporating a slit structure into the rotating component induces core loss, which contributes to an enhanced holding force.

5. Conclusions

This paper presents the development of an output-variable permanent-magnet electromagnetic hybrid brake to enhance system efficiency. A principle for compensating the braking force was proposed by inducing core loss to secure an additional holding force

when needed and varying the braking force according to the load characteristics using a lower AlNiCo permanent magnet. The stator and rotor structures were improved and the design variables were calculated to propose a design process for the brake. The proposed structure was analyzed using 2D and 3D FEA to validate the principle, derive an improved model in which core loss generates braking torque, and investigate the braking force variation mechanism. Finally, the feasibility of the design was confirmed through prototype manufacturing and experimental tests.

Author Contributions: Conceptualization, Y.-J.P.; methodology, Y.-J.P.; software, K.-D.L.; validation, K.-D.L.; formal analysis, D.-H.J.; investigation, D.-H.J.; resources, Y.-J.P.; data curation, J.-K.L.; writing—original draft, Y.-J.P.; writing—review and editing, D.-H.J.; visualization, D.-H.J.; supervision, J.-K.L.; project administration, K.-D.L.; funding acquisition, J.-K.L. All authors have read and agreed to the published version of the manuscript.

Funding: This work was supported by the Korea Institute of Energy Technology Evaluation and Planning (KETEP) funded by the Korean Government (MOTIE) through the Development and Demonstration of an Integrated Energy and Environment Management System (EEMS) for Manufacturing under Grant 2022202090003B.

Data Availability Statement: The data are contained within the article.

Conflicts of Interest: Author Yeji Park was employed by the company ECL-TECH Corp. The remaining authors declare that the research was conducted in the absence of any commercial or financial relationships that could be construed as a potential conflict of interest.

References

1. Yasa, Y.; Sincar, E.; Ertugrul, B.T.; Mese, E. Design considerations of electromagnetic brakes for servo applications. In Proceedings of the 2014 IEEE 23rd International Symposium on Industrial Electronics (ISIE), Istanbul, Turkey, 1 June 2014.
2. Lequesne, B. Dynamic model of solenoids under impact excitation, including motion and eddy currents. *IEEE Trans. Magn.* **1990**, *26*, 1107–1116. [CrossRef]
3. Vekara, T.T.; Eriksson, J.-T.; Tanttu, J.T. Dynamic model of an electromagnetic massive core brake actuator. *IEEE Trans. Magn.* **1996**, *32*, 1970–1974. [CrossRef]
4. Yao, M.; Miao, J.; Cao, S.; Chen, S.; Chai, H. The structure design and optimization of electromagnetic-mechanical wedge brake system. *IEEE Access* **2020**, *8*, 3996–4004. [CrossRef]
5. Shin, H.-J.; Choi, J.-Y.; Cho, H.-W.; Jang, S.-M. Analytical Torque Calculations and Experimental Testing of Permanent Magnet Axial Eddy Current Brake. *IEEE Trans. Magn.* **2013**, *49*, 4152–4155. [CrossRef]
6. Mohammadi, S.; Mirsalim, M.; Vaez-Zadeh, S.; Talebi, H.A. Analytical Modeling and Analysis of Axial-Flux Interior Permanent-Magnet Couplers. *IEEE Trans. Ind. Electron.* **2014**, *61*, 5940–5947. [CrossRef]
7. Yazdanpanah, R.; Mirsalim, M. Design of robust speed and slip controllers for a hybrid electromagnetic brake system. *IET Electr. Power Appl.* **2015**, *9*, 307–318. [CrossRef]
8. Yazdanpanah, R.; Mirsalim, M. Hybrid electromagnetic brakes: Design and performance evaluation. *IEEE Trans. Energy Convers.* **2015**, *30*, 60–69. [CrossRef]
9. Li, J.; Yang, G.; Fan, Y. Modeling and optimization of tubular linear permanent magnet eddy current brake with Halbach array. *Int. J. Appl. Electromagn. Mech.* **2020**, *66*, 91–113. [CrossRef]
10. Li, H.; Yang, M.; Hao, W. Research of novel eddy-current brake system for moving-magnet type linear electromagnetic launchers. In Proceedings of the 2019 Cross Strait Quad-Regional Radio Science and Wireless Technology Conference (CSQRWC), Taiyuan, China, 18–21 July 2019.
11. Wang, J.-B.; Li, Y.-H.; Yan, L.-G. Study on applying the linear Halbach array to eddy current brake system. *Int. J. Appl. Electromagn. Mech.* **2010**, *33*, 111–118. [CrossRef]
12. Kou, B.; Zhang, H.; Yin, X.; Zhou, Y.; Li, C. Research on Long Stroke Moving Secondary Permanent Magnet Linear Eddy Current Brake. *CES Trans. Electr. Mach. Syst.* **2019**, *3*, 19–29. [CrossRef]
13. Choo, K.-M.; Won, C.-Y. Design and Analysis of Electrical Braking Torque Limit Trajectory for Regenerative Braking in Electric Vehicles With PMSM Drive Systems. *IEEE Trans. Power Electron.* **2020**, *35*, 13308–13321. [CrossRef]
14. Chowdhury, A.; Islam, S.M.M. Design and Fabrication of an Automotive Electromagnetic Braking System. In Proceedings of the 2022 4th International Conference on Sustainable Technologies for Industry 4.0 (STI), Dhaka, Bangladesh, 17 December 2022.

15. D'Andrea, M.; Di Domenico, G.; Macera, D.; Fiume, F. Electromagnetic brakes in electromechanical actuators for aerospace applications. In Proceedings of the 2020 International Symposium on Power Electronics, Electrical Drives, Automation and Motion (SPEEDAM), Sorrento, Italy, 24 June 2020.
16. Mitobe, K.; Suzuki, K.; Sekiya, A.; Koyama, S.-J.; Capi, G. A soft and vibration-free positioning controller for series elastic tendon-driven robots by using gyro sensor and electromagnetic brakes. In Proceedings of the 2023 IEEE International Symposium on Robotic and Sensors Environments (ROSE), Tokyo, Japan, 6 November 2023.
17. Huang, D. Multi-Physical Field Theory Analysis of Electromagnetic Brake Rotor Disc in Automobile Integrated Braking System. In Proceedings of the 2021 IEEE Asia-Pacific Conference on Image Processing, Electronics and Computers (IPEC), Dalian, China, 14 April 2021.
18. Kou, B.; Jin, Y.; Zhang, H.; Zhang, L.; Zhang, H. Nonlinear analytical modeling of hybrid-excitation double-sided linear eddy-current brake. *IEEE Trans. Magn.* **2015**, *51*, 8003404. [CrossRef]
19. Zhang, K.; Shang, H.; Xu, J.; Niu, J.; Yue, Y. Self-Excited, Electromagnetic Braking and Heating System for Electric Buses. *IEEE Trans. Veh. Technol.* **2022**, *71*, 12543–12551. [CrossRef]
20. Heisler, H. *Advanced Vehicle Technology*, 2nd ed.; Science Direct: London, UK, 2002; pp. 450–509.
21. Yamazaki, K.; Seto, Y. Iron loss analysis of interior permanent-magnet synchronous motors-variation of main loss factors due to driving condition. *IEEE Trans. Ind. Appl.* **2006**, *42*, 1045–1052. [CrossRef]
22. Yamazaki, K.; Fukushima, Y.; Sato, M. Loss Analysis of Permanent-Magnet Motors With Concentrated Windings—Variation of Magnet Eddy-Current Loss Due to Stator and Rotor Shapes. *IEEE Trans. Ind. Appl.* **2009**, *45*, 1334–1342. [CrossRef]
23. *IEC 60034-2-1:2024*; Rotating Electrical Machines—Part 2-1: Standard Methods for Determining Losses and Efficiency from Tests (Excluding Machines for Traction Vehicles). International Electrotechnical Commission: Geneva, Switzerland, 2024. Available online: https://webstore.iec.ch/en/publication/67756 (accessed on 8 January 2025).

Disclaimer/Publisher's Note: The statements, opinions and data contained in all publications are solely those of the individual author(s) and contributor(s) and not of MDPI and/or the editor(s). MDPI and/or the editor(s) disclaim responsibility for any injury to people or property resulting from any ideas, methods, instructions or products referred to in the content.